Euro-Mediterranean Journal for Environmental Integration
https://doi.org/10.1007/s41207-023-00423-w

ORIGINAL PAPER

The geoenvironmental factors influencing slope failures in the Majerda basin, Algerian-Tunisian border

Ismail Arif[1,2,7] · Riheb Hadji[4,5,7] · Younes Hamed[2,3,7] · Noureddine Hamdi[1] · Matteo Gentilucci[6] · Soumaya Hajji[7,8,9]

Received: 15 July 2023 / Accepted: 8 September 2023

Abstract

In mountainous regions globally, landslides pose severe threats to both human lives and infrastructure, with the Mediterranean region, in particular, being highly susceptible to these destructive events that result in substantial damage to settlements and infrastructure. In this study, we employ a GIS-based approach to comprehensively characterize terrain instabilities along the Algerian-Tunisian border, recognizing the critical need for effective land planning and disaster mitigation strategies in this context. Our methodology integrates geological, geophysical, and geotechnical reconnaissance techniques and multi-criteria analysis, with a particular focus on geotechnical parameters. Our findings reveal significant slope instability within the study area; it is particularly concentrated in the mid-altitude slopes of the eastern basin, with high and very high susceptibility zones covering 20.89% of the study area. Validation of our model through ROC analysis demonstrates its high accuracy, with an area under the curve (AUC) value of 0.92. Crucially, slope gradients and precipitation emerge as key contributors to landslide occurrence, alongside Triassic lithofacies, which is a significant geological factor influencing susceptibility. These results emphasize the necessity of identifying high-landslide-susceptibility regions for sustainable land management and risk reduction, which will ultimately enhance the resilience of the studied region and mitigate the associated natural hazard risks.

Keywords Landslides · Mediterranean region · GIS-based approach · Terrain instabilities · Geotechnical parameters

Responsible Editor: João Miguel Dias.

✉ Riheb Hadji
hadjirihab@yahoo.fr

Ismail Arif
labo_geo@yahoo.fr

Younes Hamed
hamed_younes@yahoo.fr

Noureddine Hamdi
hamdinoureddine@yahoo.fr

Matteo Gentilucci
matteo.gentilucci@unicam.it

Soumaya Hajji
soumaya.hajji06@gmail.com

1 Higher Institute of the Sciences and Techniques of Waters of Gabès (ISSTEG), University of Gabes, Gabes, Tunisia

2 Laboratory for the Application of Materials to the Environment, Water and Energy (LAM3E), Faculty of Science of Gafsa, University of Gafsa, 2112 Gafsa, Tunisia

3 Department of Earth Sciences, Faculty of Sciences of Gafsa, University of Gafsa, Gafsa, Tunisia

4 Department of Earth Sciences, Institute of Architecture and Earth Sciences, Farhat Abbas University, Setif 1 University, Setif, Algeria

5 Laboratory of Applied Research in Engineering Geology, Geotechnics, Water Sciences, and Environment, University of Farhat Abbas, Setif, Algeria

6 School of Science and Technology, Geology Division, University of Camerino, Camerino, Italy

7 International Association of Water Resources in the Southern Mediterranean Basin, Gafsa, Tunisia

8 Water, Energy and Environment Laboratory (LR3E), National School of the Engineers, B.P.W.3038, Sfax, Tunisia

9 Department of Earth Sciences, Faculty of Sciences of Sfax, University of Sfax, Sfax, Tunisia

Published online: 02 November 2023

Introduction

Landslides constitute a significant global concern, as they lead to annual economic losses estimated at approximately $10 billion (World Bank 2019). These financial implications result from the widespread destruction of infrastructure, property, and agricultural crops as well as disruptions to transportation systems caused by landslides (Petley et al. 2010; Althuwaynee et al. 2016; Dahoua et al. 2018; Kaya and Midilli 2020; Nseka et al. 2021). Beyond their economic toll, landslides exact a human cost, often resulting in loss of life and forced displacement of communities (Tanyaş et al. 2017). According to the International Consortium on Landslides (ICL), landslides are responsible for an estimated 4500 fatalities annually worldwide (Klose et al. 2018). These sobering statistics underscore the paramount importance of comprehensively understanding and effectively managing landslide risks to safeguard lives and mitigate the substantial economic consequences associated with these geological hazards (Lee 2013; Gadri et al. 2015; Froude and Petley 2018; Achour and Pourghasemi 2020; Ozturk et al. 2022).

Landslides are regarded as one of the most destructive natural occurrences in the mountainous areas of the Mediterranean basin, alongside earthquakes. With their diverse geological formations, these areas are highly susceptible to landslides due to their complex tectonic history, steep terrain, and the Mediterranean climate, which is characterized by seasonal rainfall. These factors frequently result in soil saturation during the wet season, elevating the risk of slope failures. Numerous studies have been conducted to address this issue; these have focused on comprehensive geological investigations, early warning systems, land-use planning, and sustainable land management practices to reduce the associated risks and bolster the region's resilience to these geological hazards. However, it's worth noting that deterministic geotechnical studies, involving precise in-situ and laboratory testing, remain relatively scarce in this context, highlighting the need for more rigorous scientific research in this area (Hadji et al. 2014b; Zahri et al. 2016; Mouici et al. 2017; Dahoua et al. 2017a, b; Achour et al. 2017; Manchar et al. 2018; Kallel et al. 2018; Karim et al. 2019; Zeqiri et al. 2019; Fredj et al. 2020; Saadoun et al. 2020; Boubazine et al. 2022; Taib et al. 2023; Brahmi et al. 2023).

Over recent decades, the northeastern regions of Algeria and the northwestern regions of Tunisia have witnessed substantial economic losses attributable to landslides (Hadji et al. 2016; Anis et al. 2019). This predicament has been further compounded by population expansion and heightened demands for infrastructure development in hilly terrains. Consequently, the anticipation and mitigation of future landslides in these areas have assumed paramount importance in efforts to safeguard against landslide-induced damage and foster sustainable development (Tien Bui et al. 2019). The fundamental premise underlying landslide susceptibility assessment is the identification of potential combinations of factors that could lead to slope instability within a specific geographical area. Accordingly, the examination of these influential factors and their historical relationships with past landslide occurrences lays the groundwork for the predictive modeling of future landslide events (Sassa and Canuti 2008; Pradhan 2013).

The susceptibility of a slope to landslides is a complex interplay of multiple factors, encompassing the lithofacies, the slope angle, the presence of water or groundwater, and the nature of the vegetation cover present. In general, slopes characterized by steep angles and sparse vegetation exhibit heightened vulnerability to landslides, in contrast to gentler slopes with dense vegetation. Nevertheless, it's crucial to underscore that the interaction between these controlling factors can be intricate and highly site specific. Furthermore, landslides can be triggered by a diverse array of factors, including but not limited to intense rainfall, seismic activity, and anthropogenic interventions like construction or excavation. Understanding this multifaceted landscape of influences is paramount for effective landslide susceptibility assessment and risk mitigation strategies (Hungr et al. 2014; Guzzetti et al. 2022; Rahardianto et al. 2017).

A comprehensive exploration of the academic literature on landslide prediction and management reveals a diverse array of techniques for assessing susceptibility to geological hazards, prominently including landslides (Guzzetti 2021). These methodologies encompass quantitative, semiquantitative, and qualitative approaches offering a direct or indirect means of estimating and zoning landslide susceptibility. Within the quantitative realm, methods span heuristic direct estimation as well as deterministic, statistical, and probabilistic models. Notably, a plethora of bivariate and multivariate techniques, including frequency ratio (FR), linear indexing (LI), weights of evidence (WoE), an artificial neural network (ANN), logistic regression (LR), and the analytic hierarchy process (AHP), among others, are at the disposal of researchers and practitioners (Conforti and Ietto 2021). The remarkable diversity of methodological options underscores the efficacy of harnessing GIS techniques to assess and categorize landslide hazards (Goetz et al. 2015; Juliev et al. 2019). Furthermore, with the advent of artificial intelligence (AI) and data mining (DM) techniques, the domain of landslide susceptibility assessment stands poised to attain unprecedented levels of relevance and validity (Zêzere et al. 2017; Reichenbach et al. 2018; Achour et al. 2021).

However, it is imperative to recognize that each method operates based on distinct data factors and parameters for

calculation, each replete with its own set of advantages, disadvantages, and degrees of uncertainty (Šilhán 2020; Shano et al. 2020; Merghadi et al. 2020; Pham et al. 2021; Kumar et al. 2021). The efficacy of each of these models is contingent upon the chosen methodology, the quality of the underlying data, and the comprehensiveness of the field inventory of landslides.

Notably, the potential for refining susceptibility assessments lies in obtaining deterministic data pertaining to landslide occurrences, including geotechnical properties and hydrogeological characteristics. Additionally, access to large-scale lithofacies maps facilitating the petrographic characterization of intermediate rocks, which are often absent in conventional medium-scale geological maps, could significantly enhance the outcomes. By improving data quality, the performance of susceptibility assessments can be bolstered, facilitating the development of more robust models finely attuned to the unique conditions of the study area.

In our study, we opted for a logistic regression-based approach because LR is a statistical method that is commonly used to predict the probability of a binary outcome based on one or more predictor variables (Kadavi et al. 2019). The strength of this methodology is rooted in the application of well-established geospatial tools and statistical techniques. Specifically, the integration of GIS and logistic regression (LR) offers a robust framework for landslide susceptibility mapping. GIS serves as a versatile platform for the manipulation, visualization, and analysis of spatial data, while logistic regression, a proven statistical method for modeling binary outcomes, enhances the modeling process. Furthermore, the utilization of ArcGIS 10.8 and Xlstat Pro software contributes to the reliability and precision of data compilation and statistical analysis. The method's structured three-step framework, encompassing a landslide inventory, factor preparation, logistic regression modeling, and comprehensive validation through success rate and prediction rate curves, as well as the calculation of the area under the receiver operating characteristic (ROC) curve (AUC), exemplifies a systematic and transparent approach to assessing landslide susceptibility. Nonetheless, this methodology does exhibit limitations, particularly in situations involving inaccessible terrains. A noteworthy challenge that persists is the management of uncertainty and the assurance of data representativeness, which is essential for addressing the intrinsic heterogeneity and irregularities encountered in real-world terrain conditions. In the realm of landslide hazard prediction, logistic regression (LR) proves invaluable for modeling the intricate relationship between various environmental factors (such as slope angle, lithofacies, and precipitation) and the probability of landslide occurrence in specific regions. Through the analysis of these contributing factors, LR facilitates the identification of areas with heightened susceptibility to landslides, thereby enabling the implementation of targeted and effective hazard mitigation strategies. The precision of the LR model hinges on the quality and quantity of the data utilized, in addition to the judicious selection of appropriate predictor variables. Numerous studies have harnessed the LR approach for landslide hazard assessment, underscoring its utility in this domain (Pourghasemi et al. 2018).

Furthermore, the integration of statistical models into landslide hazard mapping endeavors serves the dual purpose of uncovering the underlying factors that drive landslide occurrences, including soil type, slope characteristics, and precipitation patterns. This invaluable insight informs critical decisions related to land-use planning, zoning, and the establishment of early warning systems, all of which contribute to enhancing community resilience in the face of landslide risks.

The core objective of this research is to employ a multivariate LR technique to classify areas exhibiting the highest probability of slope instability. The robustness of this model lies in its reproducibility and objective nature, enabling the quantification of landslide occurrence likelihood. Consequently, our study encompasses three principal stages: (i) the identification and cataloging of landslides, encompassing key parameters like size, location, and displacement; (ii) the mapping and evaluation of factors contributing to slope instability, culminating in the development of a comprehensive geodatabase; and (iii) the assessment and validation of a probabilistic model aimed at prioritizing the spatial distribution of landslide susceptibility within the study area. Upon completion, this research will furnish invaluable insights into the varying degrees of susceptibility to landslides in the Algerian-Tunisian border region, while also considering temporal and spatial probabilities. The utilization of statistical models, exemplified by LR, holds profound practical implications. By accurately predicting the likelihood of landslides in specific regions, planners and decision-makers are equipped to gain a deeper understanding of the associated risks and are better prepared to mitigate these geological hazards. The identification of high-risk areas allows for more efficient resource allocation, minimizing the potential for damage, injuries, or loss of life.

General setting of the study area

The Medjerda upstream basin is situated in north-eastern Algeria and spans longitudes 374,546 to 447,001 E and latitudes 3,991,989 to 4,033,586 N (WGS84-UTM32N) (Fig. 1). The area encompasses 21 municipalities, namely Mechroha, Ain Zana, Ouled Driss, Ouled Moumen, Ouilen, Khedara, Souk Ahras chief-town, Hanancha, Zaarouria, Merahna, Haddada, Khemissa, Tifech, Taoura, Sidi Fredj, Ragouba, Drea, and Mdaourouch belonging to the province

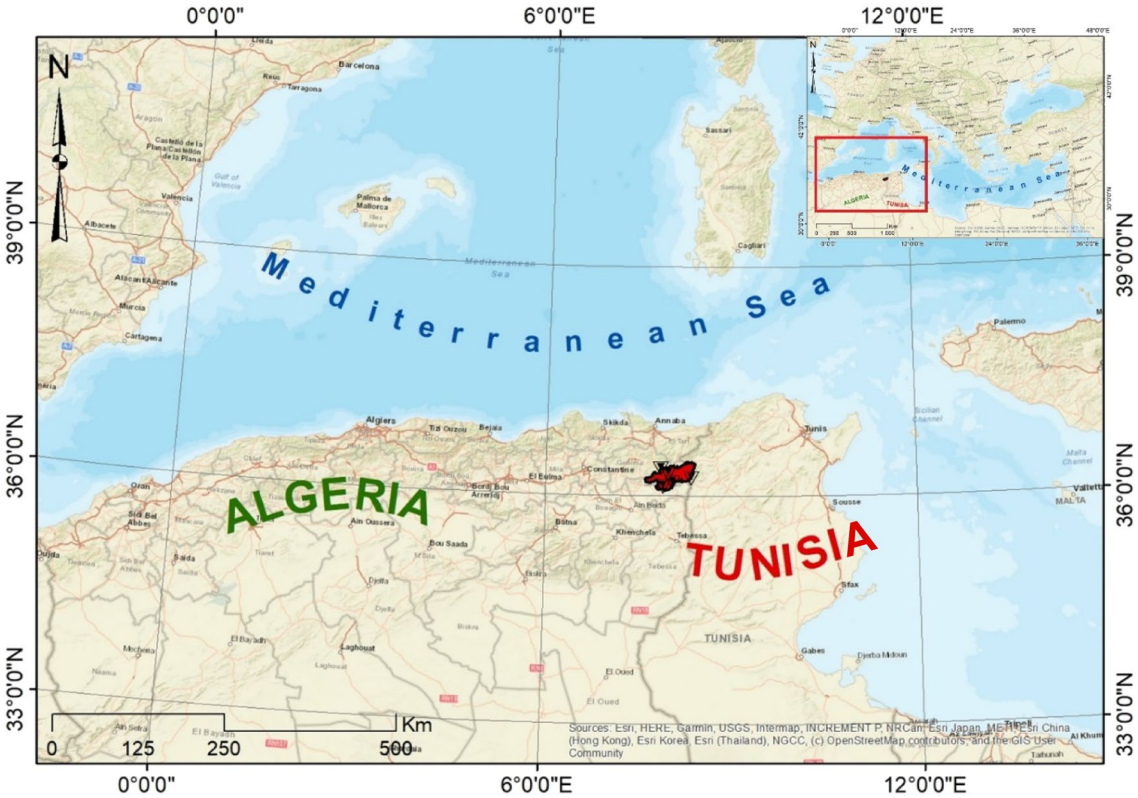

Fig. 1 Geographic situation of the Medjerda watershed

of Souk-Ahras as well as Hammam Nbail, Oued Cheham, and Dahouara belonging to the province of Guelma. The study area covers 1481 km^2 and is located in a deep valley surrounded by high mountains with a complex rocky relief that is typical of the Tell Atlas region. The total population of this area is around 323,327 people, who reside in scattered settlements and villages on the steep slopes of the mountains. The region is affected by various types of landslides, and its altitude ranges from 228 to 1373 m above sea level.

The study area, located in north-eastern Algeria on the international border, has a temperate continental climate with a Mediterranean influence that is characterized by hot and dry summers and cold wet winters, as per the Köppen–Geiger classification (Zeroual et al. 2019). The average annual temperature is 17 °C, and the inter-annual rainfall variation ranges from 400 mm/year in the south to over 633 mm/year in the north. The irregular downpours have resulted in deep gullies on the soil surface, and heavy rainstorms are usually associated with most of the landslides that have been recorded. The hydroclimatology of the Algerian-Tunisian border has been studied by various researchers, and they have discovered that this region is experiencing a significant imbalance in its hydrological system. As a result, there has been an increase in the disruption of rainfall patterns (Nekkoub et al. 2020; Brahmi et al. 2021; Besser et al. 2021; Ncibi et al. 2021; Hamed et al. 2022).

Geologically, the area is part of the Tellian chain, with geological layers that have irregular contacts and are cut by normal faults (Tamani et al. 2019). Steep slopes and carbonate rock units characterize the structural setting. The lithological facies are composed of Triassic gypsum-clay, Cretaceous marls, clay, and limestone; Eocene clay marls, limestone, marls, and sandstones; and Neogene clays and marls. The Mio-Pliocene is composed of clay, gravel, sand, silt, and unconsolidated deposits (Fig. 2). The lithologies have varying degrees of susceptibility to landsliding, depending on their characteristics and geological properties (Mahleb et al. 2022; Dib et al. 2022; Zighmi et al. 2023):

- *Triassic gypsum-clay formation*. This formation is composed of gypsum and clay, which can be prone to landsliding when saturated with water due to their low permeability. Gypsum-rich layers can be particularly problematic as gypsum is soluble in water and can create voids and weaknesses in the formation over time, increasing the risk of landslides.
- *Cretaceous marls, clay, and limestone*. Marls and clays are typically highly susceptible to landsliding when they become saturated, as they retain water and lose

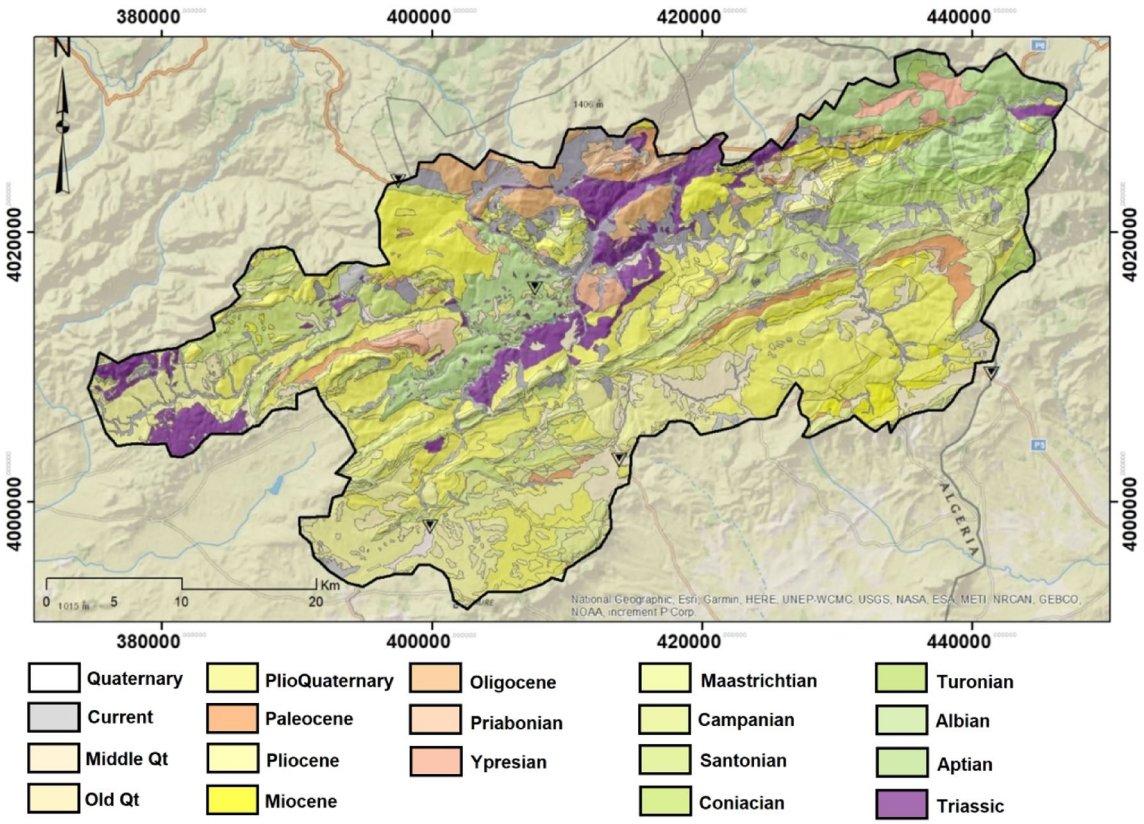

Fig. 2 Lithological map of the study area

their cohesion. Limestone layers may act as a sliding plane if they are interbedded with marls or clays, increasing the potential for landslides.

- *Eocene clay marls, limestone, marls, and sandstones*. Clay marls within this formation can be prone to landsliding, especially during heavy rainfall or when the water table rises. Limestone and sandstone layers may provide some stability but can also act as potential sliding planes in certain conditions.
- *Neogene clays and marls*. Clays and marls from the Neogene period are similar to those from the Eocene and Cretaceous and can be vulnerable to landsliding when saturated. The risk of landslides in this formation depends on factors such as slope angle, rainfall, and the presence of any geological discontinuities.
- *Quaternary deposits*. Quaternary deposits vary widely and include materials like alluvial sediments, glacial deposits, and loess. The susceptibility to landsliding in Quaternary deposits depends on their specific composition and local conditions. For example, alluvial deposits may be prone to landslides during heavy rainfall or riverbank erosion.

The landscape was shaped by neotectonic action, resulting in intense diapiric extrusion (Kerbati et al. 2020; Zerzour et al. 2020). The Maghrebian Atlas range, which was formed by the Alpine orogeny, experiences sporadic seismic activity.

Geological mapping reveals that the study area is influenced by four distinct fault families. The east–west- and north–south-oriented faults intersect the Plio-Quaternary formations. In contrast, the northwest–southeast- and northeast–southwest-oriented faults are older and cut across formations dating back to the Upper Miocene period. These faults are associated with the Lower Miocene phase, which led to the emplacement of tectonic nappe structures.

To assess the risk of landsliding in these formations more accurately, it's essential to consider local geological conditions, slope angles, groundwater levels, and any human activities that might impact stability (e.g., construction, deforestation). Geotechnical studies and engineering analyses were conducted to determine potential landslide hazards in areas with these lithological formations.

Material, methods, and data processing

A comprehensive range of investigation techniques were employed at multiple scales to obtain a thorough understanding of the terrain. Field surveys were conducted to gather detailed on-site observations and collect relevant geological data. Core drillings were performed to extract samples from different depths for further analysis and characterization. Electrical soundings were carried out to assess the subsurface electrical properties and provide insights into the geological formations and groundwater conditions. Laboratory testing played a crucial role when evaluating the physical and mechanical properties of the collected samples. This involved conducting a series of tests to determine parameters such as strength, permeability, and compressibility. The results of these tests provided valuable information for the interpretation and analysis of the site conditions. In addition to the field and laboratory investigations, terrain susceptibility mapping was undertaken to identify areas prone to instabilities and assess the potential risk of natural hazards. This mapping involved integrating various geoenvironmental factors, such as slope gradient, lithology, soil type, land cover, and hydrological characteristics, to generate a comprehensive assessment of terrain susceptibility.

Terrain reconnaissance and sampling

Geological, geophysical, and geotechnical reconnaissance activities have been initiated as part of a comprehensive program to investigate and understand various aspects of the terrain. The primary objectives of this program were assessing the seismic conditions of the area; evaluating the geophysical characteristics of the terrain; examining the geological context of the region; analyzing the geotechnical properties and conditions of the rock formations; investigating the composition and properties of Quaternary deposits; conducting a thorough analysis of the groundwater table, including its state and chemical composition; studying the hydrogeological features specific to the area of interest; assessing the geotechnical properties of the soil and rocks in the region.

These investigations aim to provide a comprehensive understanding of the terrain, allowing informed decision-making and planning for future activities or projects in the area.

The analysis of seismic conditions has provided information on the level of seismic accelerations for two different earthquake scenarios:

- *Basic probable earthquake*. This corresponds to a seismic event with a return period of 100 years and a measured seismic acceleration of $a = 0.25\ g$.
- *Maximum probable earthquake*. This represents a more severe earthquake scenario with a return period of 5000 years, with a higher projected seismic acceleration of $a = 0.32\ g$. This projection was derived by considering the earthquake that occurred on 21 Dec. 1980, which had a magnitude (M) of 5.2. Utilizing the Esteva (1968) relationship, the estimated acceleration value is $a = 0.128\ g$, which is then converted into seismic intensity.

In terms of geophysical investigations, a total of six electrical soundings were carried out, with two conducted in the mountainous bedrock and four in the valley. Through a comparison of the geoelectric models (based on the apparent electrical resistivity) with the results and logs from the soundings, it became evident that the geological structure of

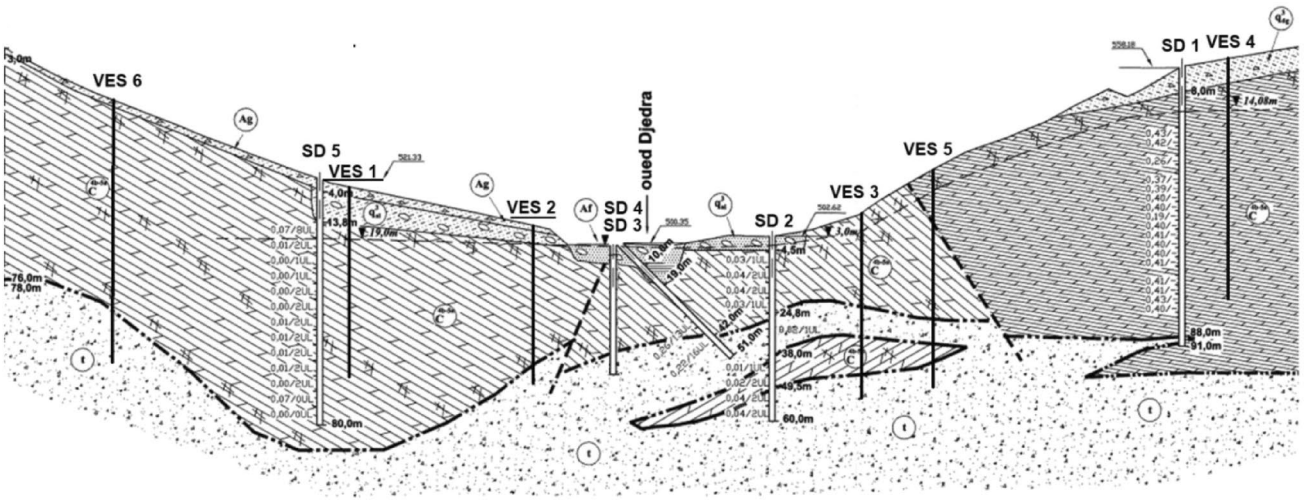

Fig. 3 Synthetic geological cross-section based on the electrical soundings (VES)

the study area's substrate is highly intricate and characterized by frequent discontinuities (Fig. 3). Notably, gypsum formations contribute significantly to this complexity, as they display pronounced diapirism. Among the ten electrical soundings conducted, five confirmed the presence of gypsum. The apparent electrical resistivity values varied considerably across the soundings. Specifically, two soundings exhibited resistivity values ranging between $\rho = 40$ Ωm and $\rho = 70$ Ωm, two others showed values ranging from $\rho = 24$ Ωm to $\rho = 32$ Ωm, and the remaining two had values of $\rho = 4$ Ωm and $\rho = 8$ Ωm. These significant variations in resistivity are attributed to the presence of clay, which leads to a decrease in apparent resistivity.

These findings shed light on the complex geological characteristics of the study area, highlighting the influential role of gypsum formations and their diapirism. Understanding the variations in resistivity is crucial for further geological analysis and planning related to the study site.

A total of 4 + 1 core drillings were carried out. The findings from SD1 provided valuable insights into the composition of the substrate beneath the Quaternary cover. It was determined that the substrate primarily consists of gray marls, which are occasionally interspersed with layers of marly limestone.

Close to the surface, the marls exhibit complete weathering and significant fracturing extending down to a depth of 12 m. However, below this depth, the marls undergo partial weathering, displaying both induration and fissuring characteristics.

These observations highlight the varying states of the marls within the subsurface, indicating the presence of weathered, altered, and fractured zones. Such information is crucial for understanding the geological conditions and their potential implications for engineering projects in the study area.

Drilling (SD2) unveiled an interesting geological feature where a mylonitic zone intersects with Triassic formations. This occurrence is attributed to the transformation of anhydrite into gypsum, leading to a significant 38% increase in bulk mass. Consequently, the layer above experiences elevated interstitial pressures, causing its degradation and material displacement. The redeposition of gypsum follows this process.

These reactions have the potential to bring about notable alterations to the overall terrain configuration. In the case of evaporites, such behavior commonly manifests as irregular disruptions within the lithological units. These disruptions are characterized by prominent mylonitic zones that emerge at the interface with heightened interstitial pressures. These observations demonstrate the unique nature of these geological processes in this zone. To address any uncertainties surrounding the precise spatial distribution of the black detrital claystones, an inclined borehole (SD4) was strategically executed. This borehole was specifically designed to intersect the targeted black detrital claystones and provide valuable insights into their geological positioning. A thorough examination of the core samples retrieved from the borehole confirmed the absence of limestone within the claystone formations. This finding is significant as it eliminates any ambiguity regarding the presence of limestone in close proximity to the claystone layers. The results obtained from this inclined borehole provide a comprehensive view of the encountered black detrital claystones and offer further evidence to support their isolated nature (i.e., the lack of any accompanying limestone deposits).

The comprehensive set of boreholes conducted yielded valuable insights. They confirmed that the degree of weathering exhibits variations corresponding to changes in depth. This phenomenon can be attributed to the influence of diapirism, which has played a significant role in shaping the geological characteristics of the area.

To further investigate these instabilities, an inclined borehole (SD5) was carefully executed, accompanied by comprehensive laboratory analyses. These analyses included tests conducted under natural wet and saturated conditions, along with the collection of samples for direct shear tests. The findings derived from these investigations provide substantial evidence that the sliding zones are sustained by the fine filtration of groundwater that accumulates within the Eocene limestone formations situated above the areas prone to landslides.

Obtaining samples from clay, marl formations, and soil requires careful attention due to their unique properties. Clay formations are known for their high plasticity and moisture retention, which can create challenges during the sampling process. To mitigate the risk of sample distortion, we utilized an auger and a split spoon sampler to penetrate the clay without causing excessive disturbance. Marl formations consist of a blend of clay and calcium carbonate and can possess varying degrees of hardness and cohesion. When extracting samples from marl, it is crucial to account for compaction levels and use appropriate coring equipment to minimize sample disturbance. Similarly, when sampling soil, factors such as soil type, texture, and moisture content must be considered to select the most appropriate technique. We used a soil auger and sometimes a hand-held core sampler to achieve minimal sample disruption. Samples were collected from formations in the vicinity of landslides (Fig. 4).

The confirmation of these findings was further strengthened by rigorous laboratory tests. These tests involved analyzing the strength parameters of the collected samples and revealed a consistent trend: as the depth increases, the values of these parameters steadily decrease. This relationship between depth and strength parameters provides essential information for assessing the stability and engineering properties of the subsurface materials.

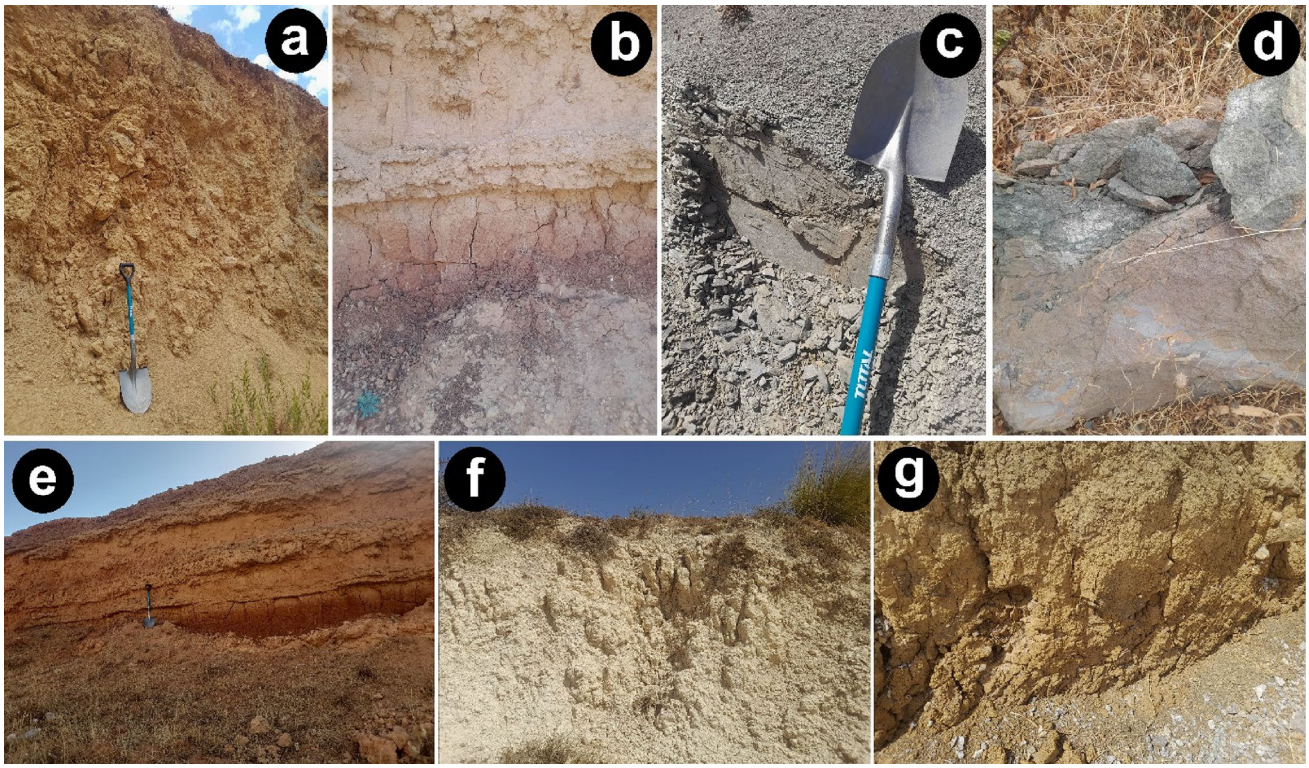

Fig. 4 Some geological outcrops that were sampled in the study zone: **a** Conglomerate facies of Oued Medjerda. **b** Carbonatic crust of Sedrata. **c** Altered marl of Hanancha. **d** Triassic green rock of Machroha. **e** Alluvium terrace of Ain Seniour. **f** Gypsum sand of Sedrata. **g** Yellow clay of Souk Ahras

Furthermore, a swelling test was specifically conducted on a reconstituted sample obtained at a depth of 44 m. This test was designed to evaluate the sample's response to changes in moisture content and applied load. It involved subjecting the sample to four cycles of loading and unloading while measuring the corresponding swelling behavior. The results obtained from the swelling test were presented graphically, allowing for a visual understanding of the swelling behavior and its relationship to the tested sample's depth.

By combining the information obtained from the boreholes, laboratory tests, and swelling tests, a more comprehensive understanding of the subsurface conditions, weathering patterns, and material properties can be achieved.

The oedometer test's stress-displacement data shows that the swelling pressure (σg) reaches 385 kPa, with a corresponding swelling index (Rg) of 0.0528.

The geological cross-sections provide a glimpse into the highly intricate geological context of the area. Notably, the presence of limestone blocks is observed as concordant bodies alternating with claystones and marls. This intricate arrangement underscores the complexity of the geological formations within the study area.

Furthermore, a rock disintegration (slake) test was conducted on a sample obtained at a depth of 41 m. The results from the test reveal that during the first cycle, the sample experienced a mass loss of 97% ($Id_1 = 3\%$), while the mass loss amounted to 99% ($Id_2 = 1\%$) in the second cycle.

These findings offer significant insights into the behavior of the tested materials under specific conditions. They shed light on the challenges posed by the complex geological features observed and provide valuable information regarding the potential strength and stability characteristics of the rock formations present in the study area.

By considering these results, a more comprehensive understanding of the geological dynamics and properties can be achieved.

Landslide inventory

For the landslide susceptibility assessments, it is essential to have information about the spatial distribution of landslides in the field to identify the causative factors. To prepare a landslide inventory map (Guzzetti et al. 1999), we collected data on historical events, satellite images, and aerial photographs and conducted field surveys. In this study, we completed and updated the landslide inventory map carried out by Hadji et al. (2013). Field reconnaissance was carried out in April 2020, April 2021, March 2022, and February 2023, and the locations and boundaries of all landslides were verified and revised using a handheld GPS. We identified a total

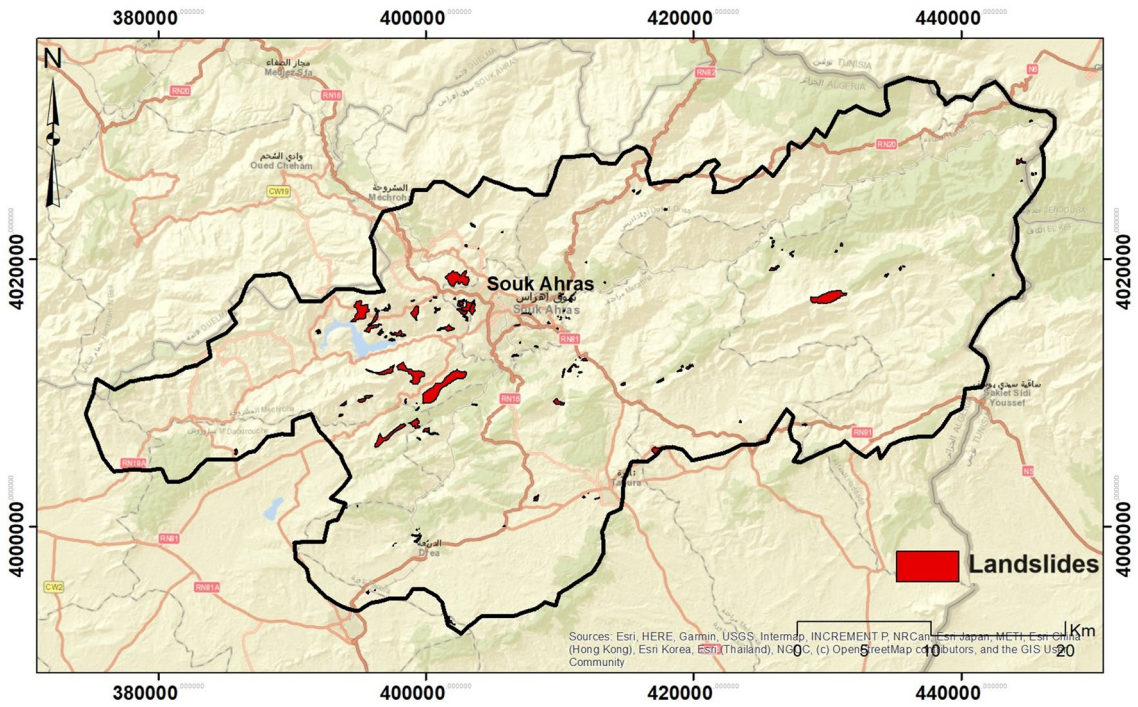

Fig. 5 Landslide inventory of the study area

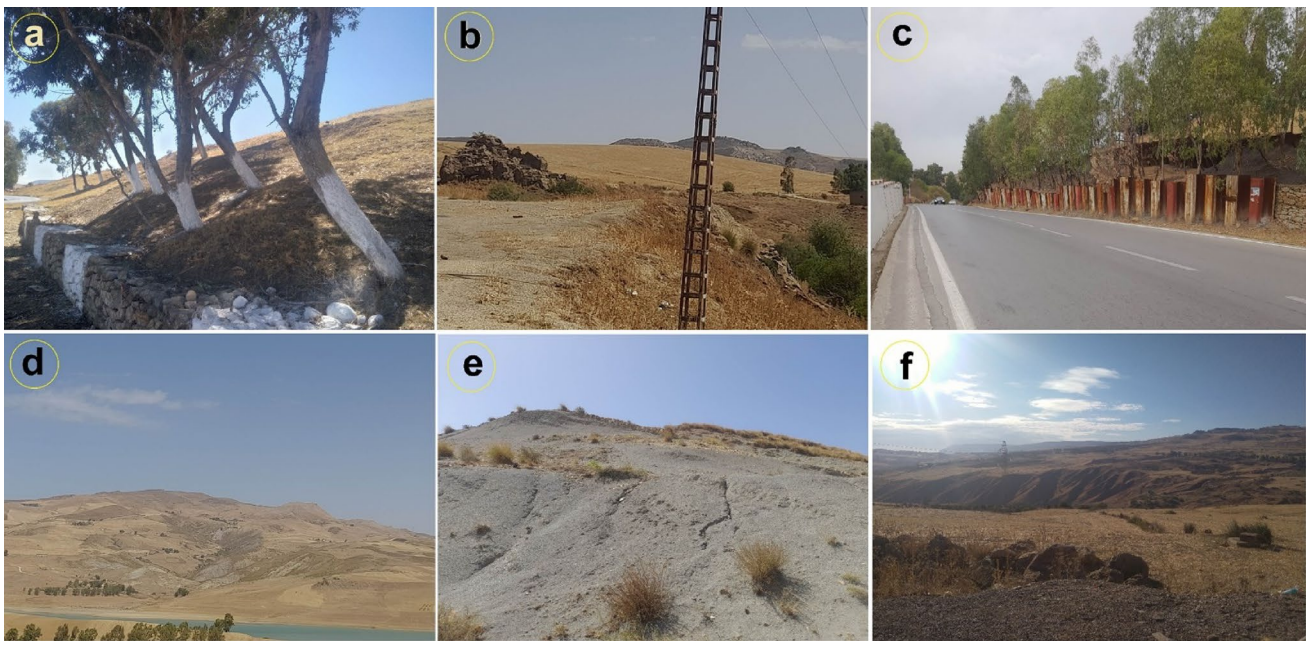

Fig. 6 Photographs of mass wasting occurrences in the study area: **a** Distorted tree trunks resembling pipes. **b** Electric poles leaning at various angles. **c** Deformed metallic sheet piles. **d** Extensive landslides. **e** Mudslides within clayey formations. **f** Rotational landslides in marl formations

of 173 landslides in the Mejerda watershed (Fig. 5), ranging in size from 681.8 m^2 to 227.52 ha. The landslides cover an area of around 1321.96 ha, which represents 0.89% of the total study area. The majority of the landslides in the study area belong to the rotational type (Fig. 6). Thorough characterizations have been conducted for the most distinctive terrain instabilities to gain deeper insights. The two primary unstable masses exhibit prominent limestone outcrops that

directly contribute to the initiation of landslides facilitated by the infiltration of both groundwater and rainfall.

Probabilistic modeling of landslide susceptibility

A method utilizing GIS and logistic (LR) regression was proposed for the zonation of landslide susceptibility in the study area (Shan et al. 2020). The data were compiled using ArcGIS 10.8 software, and statistical analysis was performed using Xlstat Pro software. Our approach for susceptibility mapping consisted of three main steps: (i) landslide inventory, data acquisition, and preparation of driving factors; (ii) processing the database by combining the factors and mapping susceptibility using logistic regression; and (iii) validating the results by creating success rate and prediction rate curves using the area under the ROC curve (AUC). To verify the susceptibility model, it was compared with a validation dataset. Our approach identified 13 key predisposing factors for landslide susceptibility zoning, including slope gradient, slope aspect, terrain elevation, lithofacies, faulting, precipitations, watercourses, road network, plan curvature, clay activity, plastic index, shear strength, and methylene blue value (Fig. 7).

In this study, our research methodology relied primarily on the utilization of the Shuttle Radar Topography Mission (SRTM) 30-m digital elevation model (DEM) as the primary data source for conducting morphological analysis. Furthermore, we employed six geological maps at a scale of 1:50,000 to collect detailed lithological information for the entire study area. To map land use across the study area comprehensively, we conducted image interpretation using Landsat 8 imagery in conjunction with ESRI basemap images. To identify and analyze landslide events, we conducted visual assessments using satellite imagery from Google Earth. Extensive fieldwork was conducted to validate and classify the observed landslides. Notably, among all the recorded landslides, only 48 occurred within urbanized areas.

Predictive variables

Assessing the likelihood of landslides in mountainous regions requires the consideration of several factors, including geological factors such as lithofacies and fault density, hydro-environmental factors like precipitation and water streams, topographic factors, including slope gradient,

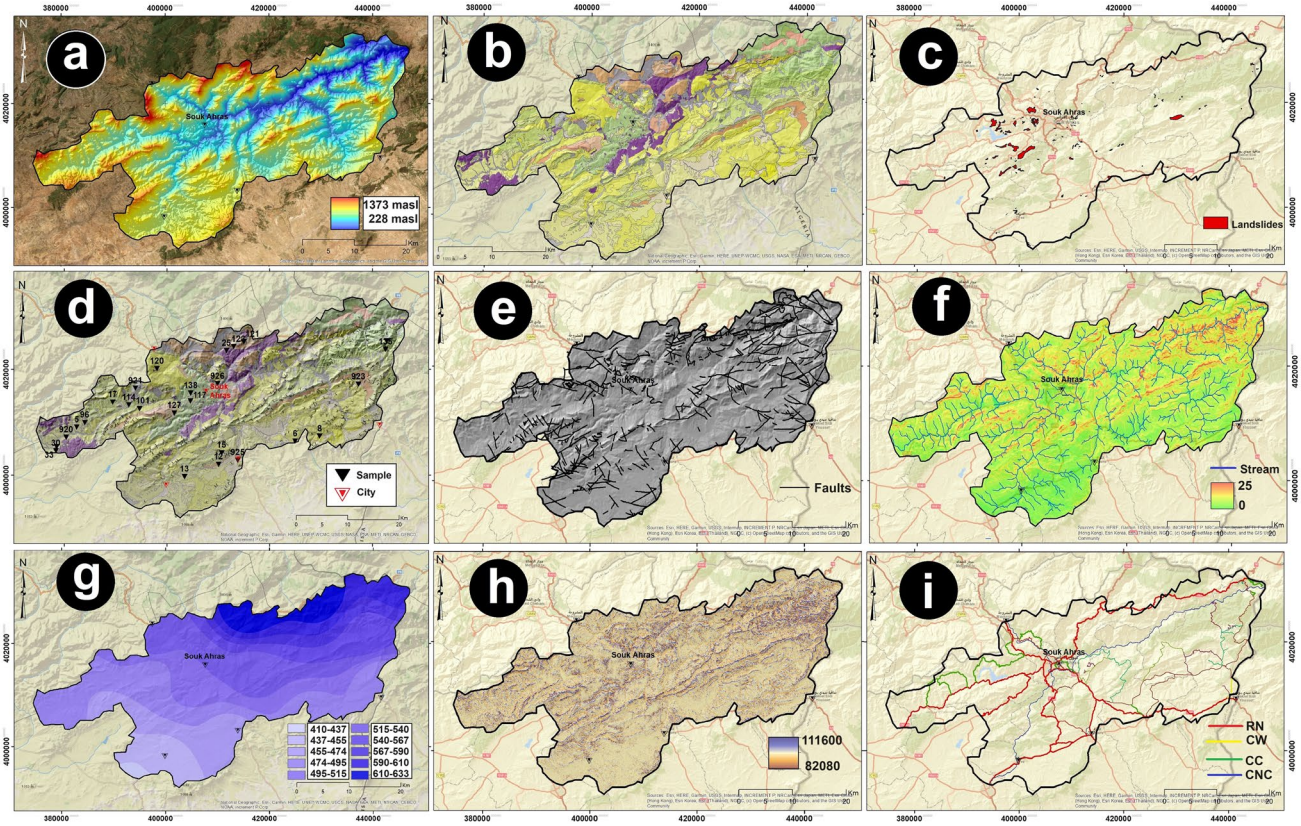

Fig. 7 Maps of variables that can be used to predict landslides in the study area, among other maps: **a** DEM, **b** lithology, **c** landslide inventory, **d** sampling map, **e** faults map, **f** slope gradient map, **g** precipitation, **h** curvature, and **i** land-use map of the study area

elevation, slope aspect, and plan curvature, as well as anthropogenic factors such as road networks and geotechnical properties such as clay activity (AC), plastic index (PI), shear strength (τ), and methylene blue value (VBS). These factors play different roles in the initiation and triggering of landslides, highlighting the importance of a comprehensive approach to their evaluation.

The lithology plays a crucial role in the genesis and triggering of landslides in mountainous regions. This is because different types of rocks and soils have different physical and mechanical properties that can affect slope stability. For instance, rocks that are highly fractured or weathered are generally weaker and more prone to failure than those that are intact and unweathered. Additionally, the presence of soluble minerals, such as gypsum or salt, can lead to the formation of cavities or dissolution channels that weaken the rock and increase the risk of landslides.

Slope gradient is another important factor that influences the occurrence of landslides. Generally, steeper slopes are more prone to landslides than gentle slopes. This is because the force of gravity acting on the soil and rock mass increases with the slope. North Africa is a region that is prone to landslides due to its complex geology and mountainous terrain. In 2003, a massive landslide occurred in the Atlas Mountains in Morocco, killing 41 people and trapping dozens more. In 2018, heavy rainfall triggered landslides in the Bechar Province of Algeria, causing significant damage to infrastructure and displacing hundreds of people. In 2019, a landslide occurred in the town of El Bayadh in western Algeria, destroying several homes and causing widespread damage. In January 2020, a rockfall happened in Aokas, Algeria, which was caused by heavy rainfall and erosion of the cliff face. The incident resulted in the death of two people and injuries to several others. The area was also evacuated as a precautionary measure.

Runoff is a crucial factor, and landslides are a common occurrence on stream banks in this watershed. To account for the impact of rivers and streams on landslides, a digital thematic map of distances from streams was created using the inverse distance weighted (IDW) interpolation technique. The map was classified into three categories based on proximity: (i) close (within 100 m), (ii) nearby (100–300 m), (iii) distant (300–500 m), and (iv) non-influential (over 500 m).

Heavy and prolonged rainfall can saturate the soil, causing it to become unstable and lose its strength. As a result, the soil is more prone to sliding down slopes, leading to landslides. Landslide initiation in the Algerian Tunisian border is strongly linked to precipitation, as highlighted by previous studies (Hadji et al. 2014a, b, 2017, 2018; Mahdadi et al. 2018; El Mekki et al. 2017; Charef et al. 2022; Ibtissam et al. 2023). To prepare a rainfall map for the study area, annual rainfall data from 2000 to 2023 obtained from 18 hydro-meteorological stations located within or near the study area via Water Balance App, were utilized. The rainfall map was classified into ten categories based on the annual total: (i) 410–473 mm/year, (ii) 473–455 mm/year, (iii) 455–474 mm/year, …, and (x) 610–633 mm/year.

Geotechnical parameters such as clay activity (AC), plastic index (PI), shear strength (τ), and methylene blue value (VBS) can have a significant impact on the spatial and temporal occurrence of landslides in mountainous regions.

Clay activity is a measure of the concentration of clay minerals in soil, which can influence the water retention and swelling properties of the soil. High clay activity can result in increased soil instability and decreased shear strength, making the area more prone to landslides.

The plastic index measures the difference in moisture content between the liquid and plastic limits of soil, which can indicate the soil's susceptibility to deformation and failure. High-plasticity soils are often associated with increased landsliding, as they can exhibit greater deformation and reduced shear strength.

Shear strength is a measure of a soil's resistance to deformation and failure when subjected to forces that cause sliding or slipping. Low-shear-strength soils can be more prone to landslides as they are more easily destabilized by external forces.

The methylene blue value is an indicator of the soil's clay mineral content and exchange capacity, which can impact the soil's water retention and swelling properties. High methylene blue values can indicate soils with high clay contents, which can be more prone to instability and landslides. Overall, geotechnical parameters play an important role in determining the spatial and temporal occurrence of landslides in mountainous regions. Understanding these parameters can help to identify areas at risk of landslides and inform effective risk management strategies.

Geotechnical parameters

Our geotechnical parameters, including clay activity (AC), plastic index (PI), shear strength (τ), and methylene blue value (VBS), were evaluated in accordance with ASTM standards and protocols (ASTM 2016, 2017, 2020, and 2021) (Table 1). Soil samples were obtained using a split-spoon sampler technique from the site, and these samples were directly transported to the laboratory for testing (Fig. 8).

The procedure for evaluating the clay activity (AC) typically involved measuring the soil's exchangeable cation content using a cation exchange resin and then calculating the activity coefficient (ASTM C837-15). For the plastic index (PI), the procedure typically involved determining the water content at which the soil transitions from a plastic to a liquid state. This can be done using the Casagrande method (ASTM D431-17). For the shear strength (τ), we performed

Table 1 Results of tests for physical properties, chemical composition analysis, and mechanical characteristics

Nature		Physical identification							Mechanical identification												Chemical analysis				
		Granulometry				Proctor		Methylene blue	Straight shear (bar)		Triaxial		Compression	Traction	Liquidity	Plasticity	Plastic index	Activity	Pc	cc	cg	Resistivity	Carbonates	% insoluble	% gypsum	Sulfate	Organic materials
Code	Lithofacies	2 mm	80 µm	60 µm	2 µm	(%)δd_{max}	Wopt (%)	VBS	Cuu	φuu°	Cuu'	φuu°'	RC	RT	WL (%)	WP (%)	IP (%)	$A = \frac{IP}{\%<2\mu}$	Preconsolidation pressure	Compressibility coefficient	Swelling coefficient	Ωm	%$CaCo_3$		$CaSO_4, 2H_2O$	% SO_4	
5	Conglomerates, gravelines, sandstone, clay, marl	86	61	35	29			2.9	0.53	19.14			–	–	46	23.11	22.89		1.34	17.61	3.28	68	12.40	87.6			2.03
6	Marl, clay, sandstone	99	80	70	30	1.63	15.80	4.5	1.03	89					76.5	34.30	62.20		2.19	29.61	5.71	54	30.80	69.2			0.81
8	Clays, marls, glauconitic sandstone	53	39	30	10.5	1.70	15.75	6.2	1.20	8					51.50	30.23	21.27		1.82	15.97	3.26	4.76	52.20	47.80			1.01
12	Marls with limestone intercalations	77	52	44	21	1.75	14.10	5.70	0.60	14.12					52	27	25		1.90	19.20	3.97	9.65	56.2	43.88			1.53
13	Marl with intercalation of marly limestone	83	60	40	18	1.80	13.40	4.80	0.71	15.10					52.67	29.10	23.57		2.10	22.40	4.05	109.46	67.10	32.90			1.30
17	Marls with small limestone beds	69	51	38	15	1.17	12.74	3.50	2.18	12.52					49.30	27.16	22.14		1.70	20.14	3.77	85.35	43.40	56.60			1.14
25	Clay-gypsum-sandstone with fragments and blocks of various rocks	91	56	48	10	1.57	18.3	3.20	0.30	23.86					59.13	35.72	32.9		1.16	26.37	4	39.29	40.10	40.10			0.94
30	Arable land. Slope formation, old alluvium, and indeterminate Quaternary	85	61	55	16	1.60	15.10	2.70	0.34	18.75					68.13	37.38	30.93		1.51	19.93	4.60	16.78	22.40	77.60			1.96

Table 1 (continued)

Nature		Physical identification							Mechanical identification													Chemical analysis				
		Granulometry				Proctor		Methylene blue	Straight shear (bar)		Triaxial		Compression	Traction	Liquidity	Plasticity	Plastic index	Activity	Pc	cc	cg	Resistivity	Carbonates	% insoluble	% gypsum	Sulfate	Organic materials
Code	Lithofacies	2 mm	80 µm	60 µm	2 µm	(%)δd_{max}	Wopt (%)	VBS	Cuu	φuu°	Cuu'	φuu°'	RC	RT	WL (%)	WP (%)	IP (%)	$A=\frac{IP}{\%<2\mu}$	Preconsolidation pressure	Compressibility coefficient	Swelling coefficient	Ωm	%$CaCo_3$		$CaSO_4, 2H_2O$	% SO_4	
33	Clay, conglomerates, sandstone, and lacustrine limestone	78	52	43.6	35.25	1.65	19.30	6.80	0.45	19.4					40.05	24.05	16.45		1.45	26.17	3.82	56.14	38	62			2.19
96	Red clays, silts	90	77	58	45	1.45	21.10	7.10	0.55	9.08					70.42	43.36	27.06		1.73	25.10	4.05	40.69	9.8	90.2			1.53
101	Clays, marls, silt stones, sandstone intercalations	70	40	84.7	19.5	1.55	18.70	0.15	0.61	15.8					58.30	27.10	31.20		1.84	19.15	3.25	57.84	58.36	41.70			0.94
114	Alluvium, pebbles, gravel, sand	45	29	16	03	1.90	10.20	0.35	0.19	31.40					36.50	22.31	14.19					140.12	6.02	93.98			2.23
120	Greenish-gray sub-Numidian clays	71	55	48	20	1.66	18.20	4.30	0.59	10.47					51.42	30.63	20.79		2.05	12.62	4.32	73.10	3.50	96.50			2.90
121	Marls with intercalations of lumachelles	98	61	45	19	1.70	15.30	3.90	0.65	23.65					45.31	27.06	18.25		1.38	23.27	3.73	91.75	49.60	50.40			1.31
123	Marl with rare limestone intercalations	67.50	50.40	38.6	20.5	1.80	13.45	5.70	0.55	22.28					55.41	33.10	22.31		1.77	20.30	3.81	133.95	66.10	33.90			1.70
127	Marls-limestones, lumachelles	93	58	43	10	1.57	16.30	3.30	0.56	22.40					50.66	27.63	23.03		1.81	14.20	2.16	196.31	74.80	25.20			1.58
135	Marl, marl-limestone, and marly limestone												632.4	45.70								328.91	86.80	13.20			

Table 1 (continued)

Nature		Physical identification							Mechanical identification												Chemical analysis				
		Granulometry				Proctor		Methylene blue	Straight shear (bar)		Triaxial		Compression	Traction	Liquidity	Plasticity	Plastic index	Activity	Pc	cc	cg	Resistivity	Carbonates	% insoluble	% gypsum	Sulfate	Organic materials
Code	Lithofacies	2 mm	80 µm	60 µm	2 µm	(%)δd_{max}	Wopt (%)	VBS	Cuu	φuu°	Cuu'	φuu°'	RC	RT	WL (%)	WP (%)	IP (%)	$A=\frac{IP}{\%<2\mu}$	Preconsolidation pressure	Compressibility coefficient	Swelling coefficient	Ωm	%$CaCo_3$		$CaSO_4, 2H_2O$	% SO_4	
137	Marls, silt stones, calcareous marly limestones												120	23.50								234.10	77.90	22.10			
921	Gravitational formations: slope scree, spreading: blocks, sands, silts					1.95	22.30	0.32							39.10	26.30	12.80		1.20	23.50	2.10	157.10	7.40	92.6			
923	Deluvio-proluvial formation: gravel, silt	40	20	4	0	2	8.30	0.25	28.40	0.80					33.93	27.08	6.85					115.4	13.5	86.5			2.10
925	Deluvio-proluvial formation: gravel, sand, silt	50	30	10	1	2.30	7.87	0.8	25.10	0.15					40.46	30.04	10.42					138.27	11.40	88.6			1.20
926	Deuivio-gravitational formations, slope scree, breccias	60	35	16	2	1.91	12.30	1.20	22.10	0.22					43.10	29.61	13.49					124.91	9.10	90.9			1.35

Fig. 8 Compositions of sampled outcrops, showcasing their material type: **a** Sandy material. **b** Silt-clayey material. **c** Silt material with organic matter. **d** Gravelly material. **e** Marly altered material. **f** Fine clayey material

a direct shear mechanic test according to standard procedures specified by ASTM D3080-20.

For the methylene blue value (VBS), the evaluation procedure involved adding a known quantity of methylene blue to the soil sample and then measuring the amount of dye adsorbed by the soil particles (ASTM D-4274-16).

Under the supervision of the Laboratory of Applied Research in Engineering Geology, Geotechnics, Water Sciences, and Environment, the tests were conducted at the Arif Geotechnical Studies Laboratory (Fig. 9).

Overall, the sampling and laboratory testing procedures for geotechnical parameters were important for accurately characterizing the properties of soil and predicting its behavior, including its potential for landslides.

Logistic regression model

The logistic regression model is a powerful tool that allows us to compile different factors that contribute to the occurrence of landslides. By using this model, we can better understand and predict the likelihood of future landslides in a given area. The model is based on the premise that these factors can lead to future events under similar conditions to those present in the past. To model landslide events, we consider them dependent variables, and the 13 factors that influence the conditions leading to the landslide are considered independent variables (Fig. 10). This technique assigns weights and coefficients to each predictor variable based on data obtained from

Fig. 9 Key laboratory tests conducted on the samples: **a** Sample preparation. **b** Shearing of marl samples. **c** The utilized triaxial compression device. **d** Samples employed in the Proctor test. **e** Weighing of the samples. **f** Sheared samples in the Casagrande box. **g** Sample preparation within the Casagrande box

samples collected in the study area. These coefficients are then used to estimate the probability of future landslides based on the presence or absence of different phenomena associated with predictor variables such as $x_1, x_2, \ldots, x_n$:

$$\text{logit}(p) = ln(p/1-p) = b_0 + b_1x_1 + b_2x_2 + \cdots + b_kx_k, \quad (1)$$

where logit(p) is the natural logarithm of the odds of the dependent variable taking a value of 1 (i.e., the log-odds or logit function). p is the probability that the dependent variable takes a value of 1. b_0 is the intercept or constant term. $b_1, b_2, \ldots, b_k$ are the coefficients of the independent variables $x_1, x_2, \ldots, x_k$, respectively. These coefficients represent the effect of each independent variable on the log-odds of the dependent variable. $1/1-p$ is the complementary probability that the dependent variable takes a value of zero.

Before implementing the model, it was necessary to create a database for each predictor variable. To obtain the values of these variables from raster layers, a binary point grid was generated. Landslide points (which indicate the occurrence of landslides) were assigned a value of 1. To balance the proportions of landslide and non-landslide grids, an equal number of points was randomly selected from regions outside the landslide zones.

Validation procedure

To validate the results obtained from the logistic regression model, a receiver operating characteristic (ROC) curve which represented the performance of the model in forecasting landslides by comparing its results with the observed field data was used. The ROC curve was constructed using landslide data that were not used when creating the susceptibility map and were reserved for validation purposes. The curve is based on threshold values that separate stable and unstable terrains. It plots specificity on the x axis and sensitivity on the y axis. Sensitivity, or the true positive rate, represents the proportion of pixels affected by landslides that were correctly classified as unstable, while specificity (or 1 − false positive rate) represents the proportion of pixels classified as stable that were actually stable. By analyzing the ROC curve, we could evaluate the performance of the model and determine its accuracy in forecasting landslides.

In order to evaluate the effectiveness of a classification model, we can use the terms TN, FP, FN, and TP. TN stands for the count of pixels that are correctly identified as not belonging to the class. FP, on the other hand, refers to the number of pixels that are mistakenly classified as

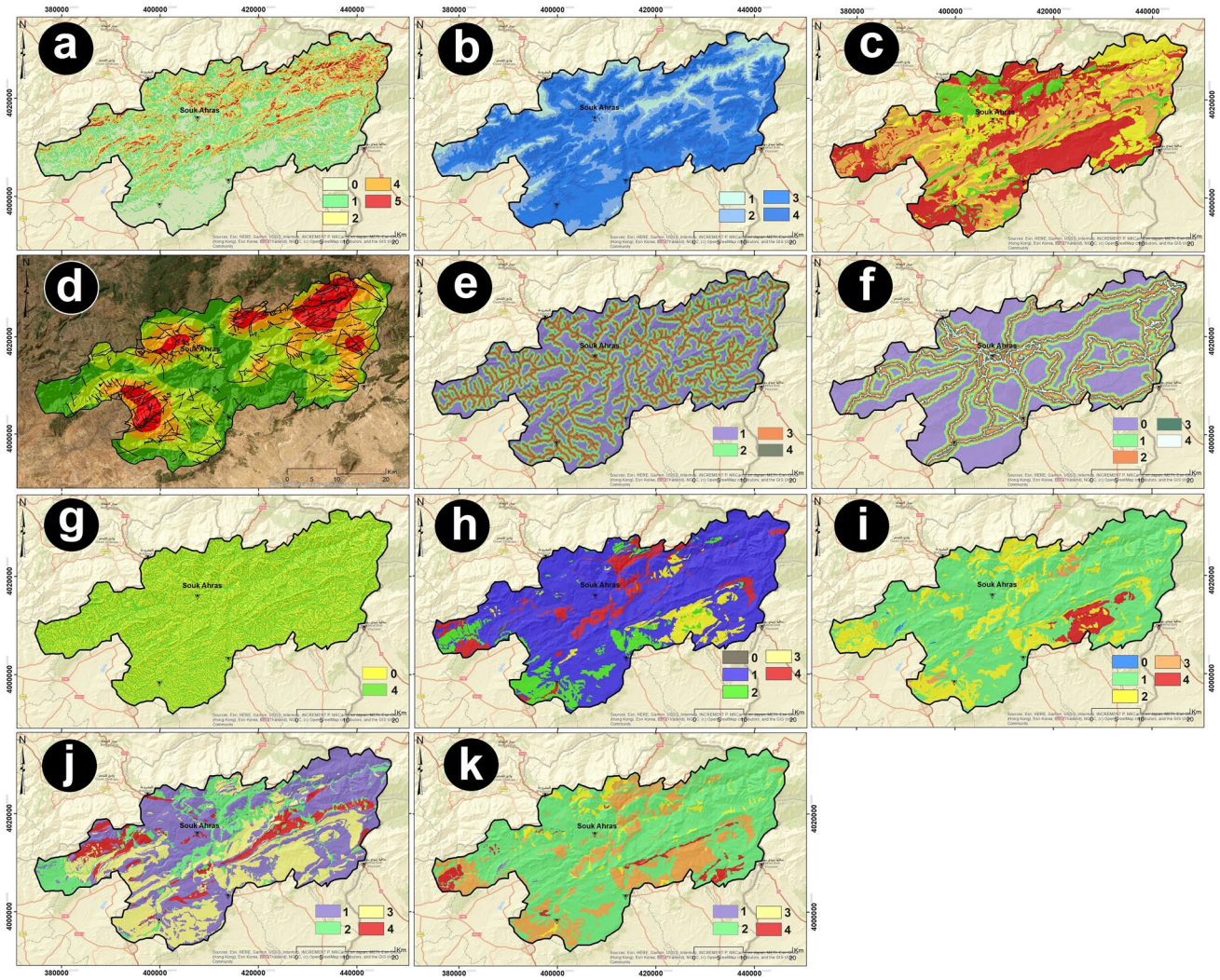

Fig. 10 Independent variables relating to the spatial occurrence of landslides in the study area: **a** reclassified slope gradient, **b** reclassified elevation, **c** reclassified lithofacies, **d** fault kernel density, **e** buffered watercourses, **f** reclassified buffered road network, **g** reclassified plan curvature, **h** reclassified clay activity (AC) **i** reclassified plastic index (PI), **j** reclassified shear strength (τ), **k** reclassified methylene blue value (VBS), **l** reclassified aspect

belonging to the class. Similarly, FN represents the number of pixels that are incorrectly classified as not belonging to the class, while TP is the count of pixels that are correctly identified as belonging to the class.

$$\text{Sensitivity} = \text{TP}/(\text{TP} + \text{FN}) \tag{2}$$

$$\text{Specificity} = 1 - \left[\text{FP}/(\text{FP} + \text{TN})\right] \tag{3}$$

A useful metric for evaluating the discriminative power of a model is the area under the curve (AUC). This metric can be used to measure the model's ability to predict the presence or absence of landslides. If the AUC is larger, the model has a stronger predictive ability. The AUC is calculated by adding up the areas of the polygons between different thresholds:

$$\text{AUC} = \int [0, 1] S(x) dF(x), \tag{4}$$

where $S(x)$ is the sensitivity of the classifier when the threshold is set at x (i.e., the true positive rate) and $F(x)$ is the false positive rate of the classifier when the threshold is set at x.

The integral is taken over the entire range of threshold values from 0 to 1.

In order to validate the results, we compared the outputs generated by the LR model with a dataset of inventoried landslides that was not used during the training phase. This

comparison allowed us to evaluate the accuracy and reliability of the models.

Results and discussion

The examination of core boxes highlighted the composition of the terrain beneath the sliding zones, revealing the presence of marly clays. This observation was reinforced by the comprehensive investigations carried out within borehole SD5. Importantly, our findings establish that, even under the circumstances of continuous groundwater infiltration, marly clays possess the potential to trigger landslides.

These findings enhance our understanding of the complex dynamics involved in terrain instability, emphasizing the significant role played by limestone formations and groundwater filtration.

LR modeling can be affected by multicollinearities between variables. To test for multicollinearity, the tolerance index (Tol) and the variance inflation factor (Vif) are commonly used. In this study, the maximum Vif and minimum Tol were 0.902 and 0.49632, respectively (Table 2), indicating that there was no multicollinearity [0.2, 2] between the independent variables. The statistical procedure allowed the selection of a varied number of predictors and offered a stepwise analysis to select the variables that best represent the model. The significance of each explanatory variable was tested using the Wald test.

The coefficients Bi (where 'i' is a natural number ranging from '$i = 0$, $i = 1$, $i = 2$...' to '$i = k$') were utilized to create the landslide susceptibility map via Eq. (1).

By analyzing the relationship between predictor variables and landslide occurrence through exp(βi), it was inferred that geological conditions, particularly the lithology and faults, can have a positive impact on landslide initiation. The results indicate that landslides tend to occur in areas dominated by Triassic clay or unconsolidated soils and that are in close proximity to faults. This finding is further supported by field observations of numerous landslides near the active fault of the Alpine orogeny and on the flanks of diapiric extrusions. Other factors such as the hydrographic network and steep slopes also play a significant role in the occurrence of landslides. Anthropogenic activities and geotechnical parameters have a moderate effect on the occurrence of these events. On the other hand, slope aspect has a minimal effect on the phenomenon.

Table 2 Multicollinearity coefficients and diagnostic indices for independent variables in the statistical procedure

Variable	Bi	W test	Exp (*B*)	Tol	Vif
Lithofacies	0.618	3.490.178	1.814	0.496	1.835
Fault density	0.399	622.756	1.448	0.502	1.157
Slope	0.408	781.696	1.462	0.788	1.617
Plan curvature	0.252	150.945	1.245	0.751	1.213
Aspect	− 0.071	16.453	0.892	0.718	1.270
Elevation	0.328	154.109	1.346	0.549	1.660
Precipitations	0.243	131.745	1.274	0.658	1.117
Distance to watercourses	0.311	155.069	1.365	0.540	1.649
Distance to roads	0.108	145.078	1.073	0.842	1.083
AC	0.081	115.493	1.084	0.711	1.261
PI	0.184	114,977	1.202	0.752	0.902
VBS	0.193	169.537	1.171	0.921	0.990
τ	0.311	526.756	1.365	0.6392	0.981
Constant	− 9.057	3.763.313	0		

We utilized the natural breaks (Jenks) method to categorize the landslide susceptibility map. Through this method, we were able to identify five probability classes: nil [0–0.113], low [113–0.182], moderate [0.182–0.432], high [0.432–0.696], and very high [0.69–1] (Fig. 11a). Based on this classification, approximately 20.89% of the area falls within high and very high susceptibility zones. Moderate susceptibility zones account for 14.46% of the total area, while the remaining 64.65% is categorized as low and nil susceptibility zones.

A comparison between the predictor variables and landslide occurrence showed that the geological conditions and geomorphology are the key influences on landslide initiation. The results indicate that areas with a high probability of landslide occurrence may require more attention and mitigation efforts to minimize the risks.

In order to validate the results of the landslide susceptibility analysis, we examined the location data of previously identified landslides that were not included in the analysis. The accuracy of the results was assessed by means of the ROC curve, which yielded an AUC value of 92.4% (Fig. 11b). This strong AUC value indicates a high level of correlation between the predictive factors and the observed landslides, supporting the accuracy of our analysis.

Conclusion and recommendations

In summary, the LR model proved to be a highly effective tool for analyzing the diverse array of factors that contribute to the genesis and initiation of landslides. By examining past landslide events, this model can identify patterns and relationships between different factors, which can be used to predict the likelihood of future landslides. This approach operates under the assumption that similar conditions in the future will lead to similar outcomes to those that occurred in the past. Our model clearly demonstrated that the occurrence of landslides is governed by a distinct set of instability factors, with the regression coefficient serving to quantify the relative contribution of each independent variable. Natural

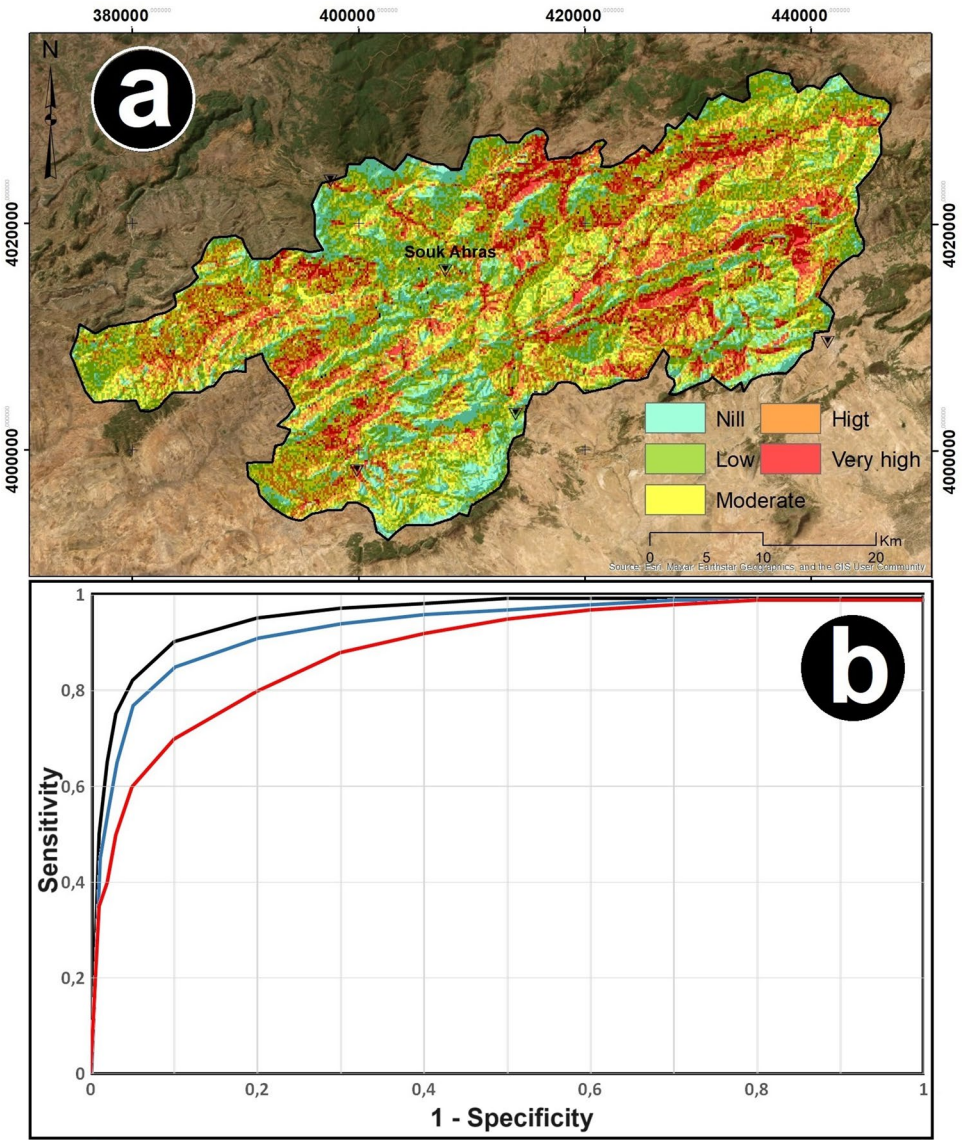

Fig. 11 **a** Landslide susceptibility zonation map generated from the LR model, and **b** ROC curve validation of the LR model

factors such as lithology, slope gradient, and drainage density were found to be more strongly correlated with landslide occurrence than other factors. However, land use, distance to faults, and elevation were found to have a moderate impact on the occurrence of landslides in this study, as evidenced by their intermediate weights.

The ROC curve and AUC provide an objective and quantitative measure of model performance. The AUC value of 92.4% is relatively high and suggests that the model has good discriminative power. The results of the validation process for the landslide susceptibility analysis indicate that the majority of the observed landslide points were located in the high and very high susceptibility classes. This finding provides strong evidence that the susceptibility map aligns well with the actual ground conditions. The map's high level of accuracy and predictive ability make it a valuable resource for informing urban planning and infrastructure development in the future, particularly in regions with similar conditions. Overall, the study's results demonstrate that the models employed in this research perform satisfactorily, and we recommend their use in further studies and practical applications.

The results obtained from our research on landslide susceptibility assessment of the Majerda basin demonstrate a remarkable consistency with findings from analogous studies conducted in the northeastern Algeria region (Hadji et al. 2013; Mahdadi et al. 2018) and the northwestern Tunisia region (Anis et al. 2019). These investigations indicate that landslides predominantly exhibit rotational behavior within the weathered zone. Furthermore, geotechnical analyses have revealed a discernible correlation between the geotechnical properties of clayey and marly formations and

the occurrence of landslides. Of particular significance is the clay fraction, a pivotal parameter in the occurrence of slope failures. An elevated clay content is associated with high soil plasticity, void ratio, and porosity values, which are concomitant with a reduction in soil cohesion. Notably, a higher water content, especially during and after intense rainfall events, exacerbates this decrease in cohesion and the friction angle, consequently diminishing the shear strength of the soil. The combined influence of the water content (characterized by heavy rainfall), the clay fraction (reflecting lithological and alteration characteristics), and the presence of steep slopes collectively control the genesis and triggering mechanisms of landslides.

Acknowledgements This work was overseen by the IAWRSMB Tunisia and the Laboratory of Applied Research in Engineering Geology, Geotechnics, Water Sciences, and Environment, Setif 1 University, Algeria. We also wish to pay tribute to the editor and reviewers for their valuable improvement of the manuscript.

Data availability The data supporting the findings of this study can be made available upon request. Researchers seeking access to the data for purposes such as replication, validation, or further analysis are welcome to do so. All we ask is that they include a proper reference to this article, in line with ethical and legal standards.

Declarations

Conflict of interest On behalf of all the authors, the corresponding author states that there is no conflict of interest. No participating authors have a financial or personal relationship with a third party whose interests could be influenced by the article's content. The corresponding author has ensured that the descriptions are accurate and agreed upon by all authors.

References

Achour Y, Pourghasemi HR (2020) How do machine learning techniques help in increasing accuracy of landslide susceptibility maps? Geosci Front 11(3):871–883. https://doi.org/10.1016/j.gsf.2019.06.004

Achour Y, Boumezbeur A, Hadji R, Chouabbi A, Cavaleiro V, Bendaoud EA (2017) Landslide susceptibility mapping using analytic hierarchy process and information value methods along a highway road section in Constantine, Algeria. Arab J Geosci 10:1–16. https://doi.org/10.1007/s12517-016-2788-8

Achour Y, Saidani Z, Touati R, Pham QB, Pal SC, Mustafa F, Balik Sanli F (2021) Assessing landslide susceptibility using a machine learning-based approach to achieving land degradation neutrality. Environ Earth Sci 80:1–20. https://doi.org/10.1007/s12665-021-09627-9

Althuwaynee OF, Pradhan B, Lee S (2016) A novel integrated model for assessing landslide susceptibility mapping using CHAID and AHP pair-wise comparison. Int J Remote Sens 37(5):1190–1209. https://doi.org/10.1080/01431161.2016.1140082

Anis Z, Wissem G, Riheb H, Biswajeet P, Essghaier GM (2019) Effects of clay properties in the landslides genesis in flysch massif: case study of Aïn Draham, North Western Tunisia. J Afr Earth Sci 151:146–152. https://doi.org/10.1016/j.jafrearsci.2019.02.019

ASTM International (2016) ASTM D4274-16: Standard test method for testing cellulose acetate (methylene blue). ASTM International, West Conshohocken. https://doi.org/10.1520/D4274-16

ASTM International (2017) ASTM D4318-17: Standard test methods for liquid limit, plastic limit, and plasticity index of soils. ASTM International, West Conshohocken. https://doi.org/10.1520/D4318-17

ASTM International (2020) ASTM D3080–20: Standard test method for direct shear test of soils under consolidated drained conditions. ASTM International, West Conshohocken. https://doi.org/10.1520/D3080-20

ASTM International (2021) ASTM C837-15(2021): Standard test method for methylene blue index of clay. ASTM International, West Conshohocken. https://doi.org/10.1520/C0837-15R21

Besser H, Dhaouadi L, Hadji R, Hamed Y, Jemmali H (2021) Ecologic and economic perspectives for sustainable irrigated agriculture under arid climate conditions: an analysis based on environmental indicators for southern Tunisia. J Afr Earth Sci 177:104134. https://doi.org/10.1016/j.jafrearsci.2021.104134

Boubazine L, Boumazbeur A, Hadji R, Kessasra F (2022) Slope failure characterization: a joint multi-geophysical and geotechnical analysis, case study of Babor Mountains range. NE Algeria Min Miner Depos 16(4):65–70

Brahmi S, Baali F, Hadji R, Brahmi S, Hamad A, Rahal O, Hamed Y (2021) Assessment of groundwater and soil pollution by leachate using electrical resistivity and induced polarization imaging survey, case of Tebessa municipal landfill, NE Algeria. Arabian J Geosci 14:1–13. https://doi.org/10.1007/s12517-020-06275-x

Brahmi S, Fehdi C, Hadji R, Brahmi S, Hamad A, Hamed Y (2023) Karst-induced sinkhole detection using a tomography imaging survey, case of Setifian high plain, NE Algeria. Geotech Geol Eng 41:1961–1976

Charef N, Berrah Y, Boumezbeur A (2022) Contribution parametric optimization study of landslides movements using statistical tools in the Region of Souk Ahras (Algeria). In: Boumezbeur A, Achour Y, Pourghasemi HR, Bensaida FK (eds) Research developments in geotechnics, geo-informatics and remote sensing: proceedings of the 2nd Springer Conference of the Arabian Journal of Geosciences (CAJG-2), Tunisia 2019. Springer International, Cham, pp 27–29. https://doi.org/10.1007/978-3-030-83755-1_5

Conforti M, Ietto F (2021) Modeling shallow landslide susceptibility and assessment of the relative importance of predisposing factors, through a GIS-based statistical analysis. Geosciences 11(8):333. https://doi.org/10.3390/geosciences11080333

Dahoua L, Savenko VY, Hadji R (2017a) GIS-based technic for roadside-slope stability assessment: an bivariate approach for A1 east-west highway, North Algeria. Mining Sci 24:81–91

Dahoua L, Yakovitch SV, Hadji R, Farid Z (2017b) Landslide susceptibility mapping using analytic hierarchy process method in BBA-Bouira Region, case study of east-west highway, NE Algeria. In: Kallel A, Ksibi M, Ben Dhia H, Khélifi N (eds) Recent advances in environmental science from the Euro-Mediterranean and surrounding regions. EMCEI 2017. Advances in Science, Technology & Innovation (IEREK Interdisciplinary Series for Sustainable Development). Springer, Cham

Dahoua L, Usychenko O, Savenko VY, Hadji R (2018) Mathematical approach for estimating the stability of geotextile-reinforced embankments during an earthquake. Mining Sci 25:207–217

Dib I, Khedidja A, Chattah W, Hadji R (2022) Multivariate statistical-based approach to the physical-chemical behavior of shallow groundwater in a semiarid dry climate: the case study of the Gadaïne-Ain Yaghout plain NE Algeria. Mining Miner Depos 16(3):38–47. https://doi.org/10.33271/mining16.03.038

El Mekki A, Hadji R, Chemseddine F (2017) Use of slope failures inventory and climatic data for landslide susceptibility, vulnerability, and risk mapping in souk Ahras region. Mining Sci 24:237–249

Esteva L (1968) Bases para la formulación de decisiones de diseño sísmico (Basis for decision-making of seismic design). Doctoral dissertation, PhD. Thesis

Fredj M, Hafsaoui A, Riheb H, Boukarm R, Saadoun A (2020) Back-analysis study on slope instability in an open pit mine (Algeria). Natsional'nyi Hirnychyi Universytet Naukovyi Visnyk 2:24–29. https://doi.org/10.33271/nvngu/2020-2/024

Froude MJ, Petley DN (2018) Global fatal landslide occurrence from 2004 to 2016. Nat Hazard 18(8):2161–2181. https://doi.org/10.5194/nhess-18-2161-2018

Gadri L, Hadji R, Zahri F, Benghazi Z, Boumezbeur A, Laid BM, Raïs K (2015) The quarries edges stability in opencast mines: a case study of the Jebel Onk phosphate mine, NE Algeria. Arab J Geosci 8:8987–8997. https://doi.org/10.1007/s12517-015-1921-7

Goetz JN, Brenning A, Petschko H, Leopold P (2015) Evaluating machine learning and statistical prediction techniques for landslide susceptibility modeling. Comput Geosci 81:1–11. https://doi.org/10.1016/j.cageo.2015.04.001

Guzzetti F (2021) On the prediction of landslides and their consequences. In: Sassa K, Canuti Y, Yamazaki F, Mikos M (eds) Understanding and reducing landslide disaster risk. Volume 1: Sendai landslide partnerships and Kyoto landslide commitment. Springer, Cham, pp 3–32

Guzzetti F, Carrara A, Cardinali M, Reichenbach P (1999) Landslide hazard evaluation: a review of current techniques and their application in a multi-scale study, Central Italy. Geomorphology 31(1–4):181–216. https://doi.org/10.1016/S0169-555X(99)00078-1

Guzzetti F, Gariano SL, Peruccacci S, Brunetti MT, Melillo M (2022) Rainfall and landslide initiation. In: Rainfall. Elsevier, pp 427–450

Hadji R, Limani Y, Baghem M, Demdoum A (2013) Geologic, topographic and climatic controls in landslide hazard assessment using GIS modeling: a case study of Souk Ahras region, NE Algeria. Quatern Int 302:224–237. https://doi.org/10.1016/j.quaint.2013.03.013

Hadji R, Limani Y, Boumazbeur AE, Demdoum A, Zighmi K, Zahri F, Chouabi A (2014a) Climate change and its influence on shrinkage–swelling clays susceptibility in a semi-arid zone: a case study of Souk Ahras municipality. NE-Algeria. Desalin Water Treat 52(10–12):2057–2072. https://doi.org/10.1080/19443994.2013.824573

Hadji R, Limani Y, Demdoum A (2014b) Using multivariate approach and GIS applications to predict slope instability hazard case study of Machrouha municipality, NE Algeria. In: 1st Int Conf on Information and Communication Technologies for Disaster Management (ICT-DM), Algiers, Algeria, 24–25 Mar 2014, pp 1–10. https://doi.org/10.1109/ICT-DM.2014.6917787

Hadji R, Chouabi A, Gadri L, Raïs K, Hamed Y, Boumazbeur A (2016) Application of linear indexing model and GIS techniques for the slope movement susceptibility modeling in Bousselam upstream basin, Northeast Algeria. Arab J Geosci 9:1–18. https://doi.org/10.1007/s12517-015-2161-7

Hadji R, Rais K, Gadri L, Chouabi A, Hamed Y (2017) Slope failure characteristics and slope movement susceptibility assessment using GIS in a medium scale: a case study from Ouled Driss and Machroha municipalities, Northeast Algeria. Arab J Sci Eng 42:281–300. https://doi.org/10.1007/s13369-016-2365-7

Hadji R, Achour Y, Hamed Y (2018). Using GIS and RS for slope movement susceptibility mapping: comparing AHP, LI and LR methods for the Oued Mellah Basin, NE Algeria. In: Recent advances in environmental science from the Euro-Mediterranean and surrounding regions: proceedings of Euro-Mediterranean Conference for Environmental Integration (EMCEI-1), Tunisia 2017. Springer International, Cham, pp 1853–1856. https://doi.org/10.1007/978-3-319-70548-4_269

Hamed Y, Hadji R, Ncibi K, Hamad A, Ben Saad A, Melki A, Mustafa E (2022) Modelling of potential groundwater artificial recharge in the transboundary Algero-Tunisian Basin (Tebessa-Gafsa): The application of stable isotopes and hydroinformatics tools. Irrig Drain 71(1):137–156. https://doi.org/10.1002/ird.2737

Hungr O, Leroueil S, Picarelli L (2014) The Varnes classification of landslide types, an update. Landslides 11:167–194

Ibtissam B, Abderrahmane B, Chemseddine F (2023) Unsaturated soil slope properties and shallow landslides development in Souk Ahras area, NE, Algeria. Arabian J Geosci 16(4):270. https://doi.org/10.1007/s12517-023-09586-0

Juliev M, Mergili M, Mondal I, Nurtaev B, Pulatov A, Hübl J (2019) Comparative analysis of statistical methods for landslide susceptibility mapping in the Bostanlik District, Uzbekistan. Sci Total Environ 653:801–814. https://doi.org/10.1016/j.scitotenv.2018.10.341

Kadavi PR, Lee CW, Lee S (2019) Landslide-susceptibility mapping in Gangwon-do, South Korea, using logistic regression and decision tree models. Environ Earth Sci 78:1–17. https://doi.org/10.1007/s12665-019-8717-0

Kallel A, Ksibi M, Dhia HB, Khélifi N (eds) (2018) Recent advances in environmental science from the Euro-Mediterranean and surrounding regions: proceedings of Euro-Mediterranean conference for environmental integration (EMCEI-1), Tunisia 2017. Springer International, Cham. https://doi.org/10.1007/978-3-319-70548-4

Karim Z, Hadji R, Hamed Y (2019) GIS-based approaches for the landslide susceptibility prediction in Setif Region (NE Algeria). Geotech Geol Eng 37(1):359–374. https://doi.org/10.1007/s10706-018-0603-3

Kaya A, Midilli ÜM (2020) Slope stability evaluation and monitoring of a landslide: a case study from NE Turkey. J Mt Sci 17(11):2624–2635. https://doi.org/10.1007/s11629-020-6279-9

Kerbati NR, Gadri L, Hadji R, Hamad A, Boukelloul ML (2020) Graphical and numerical methods for stability analysis in surrounding rock of underground excavations, example of Boukhadra Iron Mine NE Algeria. Geotech Geol Eng 38:2725–2733. https://doi.org/10.1007/s10706-020-01400-4

Klose M, Damm B, Terhorst B (2018) The global risk of landslide disasters: a global-scale assessment of landslide potential, exposure, and risk. Landslide dynamics: ISDR-ICL landslide interactive teaching tools. Springer, Cham, pp 29–55. https://doi.org/10.1007/978-3-319-57730-3_3

Kumar P, Debele SE, Sahani J, Rawat N, Marti-Cardona B, Alfieri SM, Zieher T (2021) Nature-based solutions efficiency evaluation against natural hazards: modelling methods, advantages and limitations. Sci Total Environ 784:147058. https://doi.org/10.1016/j.scitotenv.2021.147058

Lee S (2013) Landslide detection and susceptibility mapping in the Sagimakri area, Korea using KOMPSAT-1 and weight of evidence technique. Environ Earth Sci 70:3197–3215. https://doi.org/10.1007/s12665-013-2468-4

Mahdadi F, Boumezbeur A, Hadji R, Kanungo DP, Zahri F (2018) GIS-based landslide susceptibility assessment using statistical models: a case study from Souk Ahras province, NE Algeria. Arabian J Geosci 11(17):476. https://doi.org/10.1007/s12517-018-3697-1

Mahleb A, Hadji R, Zahri F, Chibani A, Hamed Y (2022) Water-borne erosion estimation using the revised universal soil loss equation (RUSLE) model over a semiarid watershed: case study of Meskiana Catchment, Algerian-Tunisian border. Geotech Geol Eng. https://doi.org/10.1007/s10706-022-02152-3

Manchar N, Benabbas C, Hadji R, Bouaicha F, Grecu F (2018) Landslide susceptibility assessment in Constantine region (NE Algeria) by means of statistical models. Stud Geotech Mech 40(3):208–219. https://doi.org/10.2478/sgem-2018-0022

Merghadi A, Yunus AP, Dou J, Whiteley J, ThaiPham B, Bui DT, Abderrahmane B (2020) Machine learning methods for landslide susceptibility studies: a comparative overview of algorithm performance. Earth-Sci Rev 207:103225. https://doi.org/10.1016/j.earscirev.2020.103225

Mouici R, Baali F, Hadji R, Boubaya D, Audra P, Fehdi CÉ, Arfib B (2017) Geophysical, geotechnical, and speleologic assessment for karst-sinkhole collapse genesis in Cheria plateau (NE Algeria). Mining Sci 24:59–71

Ncibi K, Hadji R, Hajji S, Besser H, Hajlaoui H, Hamad A, Hamed Y (2021) Spatial variation of groundwater vulnerability to nitrate pollution under excessive fertilization using index overlay method in central Tunisia (Sidi Bouzid basin). Irrig Drain 70(5):1209–1226. https://doi.org/10.1002/ird.2574

Nekkoub A, Baali F, Hadji R, Hamed Y (2020) The EPIK multi-attribute method for intrinsic vulnerability assessment of karstic aquifer under semi-arid climatic conditions, case of Cheria Plateau, NE Algeria. Arab J Geosci 13:1–15. https://doi.org/10.1007/s12517-019-4882-6

Nseka D, Mugagga F, Opedes H, Ayesiga P, Wasswa H, Mugume I, Nalwanga F (2021) The damage caused by landslides in socio-economic spheres within the Kigezi highlands of South Western Uganda. Environ Socio-Econ Stud 9(1):23–34. https://doi.org/10.2478/environ-2021-0004

Ozturk U, Bozzolan E, Holcombe EA, Shukla R, Pianosi F, Wagener T (2022) How climate change and unplanned urban sprawl bring more landslides. Nature 608(7922):262–265. https://doi.org/10.1038/d41586-022-00344-4

Petley D, Alcantara-Ayala I, Goudie AS (2010) Landslide hazards. Geomorphological hazards and disaster prevention, pp 63–74

Pham QB, Achour Y, Ali SA, Parvin F, Vojtek M, Vojteková J, Anh DT (2021) A comparison among fuzzy multi-criteria decision making, bivariate, multivariate and machine learning models in landslide susceptibility mapping. Geomatics Nat Hazards Risk 12(1):1741–1777. https://doi.org/10.1080/19475705.2021.1984172

Pourghasemi HR, Teimoori Yansari Z, Panagos P, Pradhan B (2018) Analysis and evaluation of landslide susceptibility: a review on articles published during 2005–2016 (periods of 2005–2012 and 2013–2016). Arab J Geosci 11:1–12. https://doi.org/10.1007/s12517-017-3272-6

Pradhan B (2013) A comparative study on the predictive ability of the decision tree, support vector machine and neuro-fuzzy models in landslide susceptibility mapping using GIS. Comput Geosci 51:350–365. https://doi.org/10.1016/j.cageo.2012.08.023

Rahardianto T, Saputra A, Gomez C (2017) Assessment of landslide distribution map reliability in Niigata prefecture–Japan using frequency ratio approach. In: AIP Conference Proceedings, vol 1857, No. 1. AIP Publishing

Reichenbach P, Rossi M, Malamud BD, Mihir M, Guzzetti F (2018) A review of statistically-based landslide susceptibility models. Earth Sci Rev 180:60–91. https://doi.org/10.1016/j.earscirev.2018.03.001

Saadoun A, Yilmaz I, Hafsaoui A, Hadji R, Fredj M, Boukarm R, Nakache R (2020) Slope stability study in quarries by different approaches: case Chouf Amar Quarry, Algeria. IOP Conf Ser Mater Sci Eng 960(4):042026. https://doi.org/10.1088/1757-899x/960/4/042026

Sassa K, Canuti P (eds) (2008) Landslides-disaster risk reduction. Springer, Berlin

Shan Y, Chen S, Zhong Q (2020) Rapid prediction of landslide dam stability using the logistic regression method. Landslides 17:2931–2956. https://doi.org/10.1007/s10346-020-01411-0

Shano L, Raghuvanshi TK, Meten M (2020) Landslide susceptibility evaluation and hazard zonation techniques—a review. Geoenviron Disasters 7(1):1–19. https://doi.org/10.1186/s40677-020-00163-7

Šilhán K (2020) Dendrogeomorphology of landslides: principles, results and perspectives. Landslides 17(10):2421–2441. https://doi.org/10.1007/s10346-020-01407-4

Taib H, Hadji R, Hamed Y, Bensalem MS, Amamria S (2023) Exploring neotectonic activity in a semiarid basin: a case study of the Ain Zerga watershed. J Umm Al-Qura Univ Appl Sci. https://doi.org/10.1007/s43994-023-00072-3

Tamani F, Hadji R, Hamad A, Hamed Y (2019) Integrating remotely sensed and GIS data for the detailed geological mapping in semi-arid regions: case of Youks les Bains Area, Tebessa Province, NE Algeria. Geotech Geol Eng 37(4):2903–2913. https://doi.org/10.1007/s10706-019-00976-x

Tanyaş H, van Westen CJ, Allstadt KE, Anna Nowicki Jessee M, Görüm T, Jibson RW, Godt JW, Sato HP, Schmitt RG, Marc O, Hovius N (2017) Presentation and analysis of a worldwide database of earthquake-induced landslide inventories. J Geophys Res Earth Surf 122(10):1991–2015. https://doi.org/10.1002/2017JF004265

Tien Bui D, Shahabi H, Omidvar E, Shirzadi A, Geertsema M, Clague JJ, Lee S (2019) Shallow landslide prediction using a novel hybrid functional machine learning algorithm. Remote Sens 11(8):931. https://doi.org/10.3390/rs11080931

World Bank (2019) Understanding risk: landslides. Retrieved on March 1, 2023, from https://www.worldbank.org/en/topic/disasterriskmanagement/brief/understanding-risk-landslides

Zahri F, Boukelloul M, Hadji R, Talhi K (2016) Slope stability analysis in open pit mines of jebel gustar career, NE Algeria—a multi-steps approach. Mining Sci 23:137–146

Zeqiri RR, Riheb H, Karim Z, Younes G, Rania B, Aniss M (2019) Analysis of safety factor of security plates in the mine "Trepça" Stantërg. Mining Sci 26:21

Zeroual A, Assani AA, Meddi M, Alkama R (2019) Assessment of climate change in Algeria from 1951 to 2098 using the Köppen-Geiger climate classification scheme. Clim Dyn 52(1–2):227–243. https://doi.org/10.1007/s00382-018-4242-6

Zerzour O, Gadri L, Hadji R, Mebrouk F, Hamed Y (2020) Semi-variograms and kriging techniques in iron ore reserve categorization: application at Jebel Wenza deposit. Arab J Geosci 13:1–10. https://doi.org/10.1007/s12517-020-05518-2

Zêzere JL, Pereira S, Melo R, Oliveira SC, Garcia RA (2017) Mapping landslide susceptibility using data-driven methods. Sci Total Environ 589:250–267. https://doi.org/10.1016/j.scitotenv.2017.02.183

Zighmi K, Zahri F, Hadji R, Benmarce K, Hamed Y (2023) Polymetallic mineralization hosted in the Neogene sedimentary strata of the Algerian Tellian range: a comprehensive overview. Mining Miner Depos 17(2):20–27. https://doi.org/10.33271/mining17.02.020